

Design of Synthetic Polymer Nanoparticles That Facilitate Resolubilization and Refolding of Aggregated Positively Charged Lysozyme

Masahiko Nakamoto,[†] Tadashi Nonaka,[†] Kenneth J. Shea,[‡] Yoshiko Miura,[†] and Yu Hoshino^{*,†}

[†]Department of Chemical Engineering, Kyushu University, 744 Motooka, Nishi-ku, Fukuoka 819-0395, Japan

[‡]Department of Chemistry, University of California, Irvine, Irvine, California 92697, United States

Supporting Information

ABSTRACT: Designed polymer hydrogel nanoparticles (NPs) capable of facilitating resolubilization and refolding of an aggregated protein, positively charged lysozyme, are prepared. NPs designed to interact strongly with denatured lysozyme and relatively weakly with native lysozyme, facilitated resolubilization and refolding of aggregated lysozyme. Such NPs could be prepared by copolymerizing optimized combinations and populations of functional monomers. The refolded lysozyme showed native conformation and enzymatic activity. Eleven grams of aggregated protein was refolded by 1 g of NPs. However, NPs having low affinity to denatured lysozyme and NPs having high affinity to both denatured and native lysozyme showed relatively low facilitation activity. Our results suggest a potential strategy for the design of artificial chaperones with high facilitating activity.

Denaturation and aggregation of proteins is one of the most serious problems in the utilization of proteins. Therefore, materials that stabilize the native structure of proteins and/or facilitate refolding of denatured proteins are of significant interest.

It has been reported that the thermal stability of proteins increases and the thermal aggregation is suppressed by well-designed poly(ethylene glycol) (PEG)¹ and poly(*N,N*-diethyl aminoethyl methacrylate)-*graft*-poly(ethylene glycol) (PDEAE-MA-*g*-PEG).² Increase in the stability of proteins has also been achieved by covalent conjugation of synthetic glycopolymers³ and spherical nanogel consisting of polyacrylamide.⁴ Amphiphilic nanosize gel particles consisting of polysaccharides suppress protein aggregation during the refolding process by encapsulating and isolating denatured proteins in the nanogel particles.^{5–7} However, little has been reported about materials that facilitate resolubilization and refolding of aggregated proteins.

In living cells, protein chaperones facilitate refolding of denatured proteins and/or nascent proteins.^{8,9} In order for the chaperones to facilitate refolding of proteins, it is important that chaperones effectively interact with hydrophobic domain of denatured proteins. Furthermore, chaperones have a cavity/channel that enables denatured proteins to be encapsulated.^{9–14} The encapsulated proteins are allowed to reach the most stable native conformation in the isolated environment without

reaggregating with other hydrophobic proteins. It is equally important that the native proteins have relatively weak affinity with chaperones so that the refolded proteins can be readily dissociated.¹⁴ Conformation change of chaperones induced by ATP binding, ATP hydrolysis and/or binding of cochaperones is often utilized to switch on/off the affinity of chaperones with substrate proteins.^{10,15} Some of the chaperones further facilitate resolubilization of aggregated proteins.^{11–13} To resolubilize aggregates, chaperones bind on aggregates, then detach denatured proteins and/or bind to denatured proteins that are released from aggregates. Then the captured proteins are refolded in the isolated environment, resulting in the growing population of the stable native proteins in the system.

Therefore, hydrogel nanoparticles (NPs) that can encapsulate denatured proteins with high affinity and that interact weakly with native proteins may facilitate resolubilization and/or refolding of aggregated proteins. Recently, synthetic polymer NPs that recognize target proteins/peptides via multipoint and multimodal interactions were obtained by optimizing combinations and populations of functional groups.^{16–18} The interaction can be further switched on/off by increasing/decreasing volume density of the functional group with the collapse/swell phase transition of the poly-*N*-isopropylacrylamide (PNIPAm) NPs.¹⁹ PNIPAm NPs with high affinity to native proteins at temperatures above the volume phase transition temperature suppress heat-induced protein aggregation by forming a stable complex with native proteins at high temperatures.²⁰ Dawson and co-workers reported that NPs are capable of inhibiting and temporarily reversing the fibrillation of A β protein.²¹ They also reported that depending upon the concentration of peptides and NPs, the kinetics of fibrillation could be accelerated or inhibited.²²

In this study, we aimed to design polymer NPs capable of facilitating resolubilization and refolding of an aggregated protein. Multifunctional acrylamide-based hydrogel NPs were utilized as platform. Lysozyme, a positively charged glycoside hydrolase (isoelectric point = 9.3, molecular weight = 14.3 kDa) was selected as the model substrate protein. It has been reported that small proteins as lysozyme can be encapsulated in the pNIPAm based hydrogel particles.^{23,24} NPs with various combinations of functional groups and populations were prepared. Capability of each NP to facilitate resolubilization

Received: December 2, 2015

Published: February 19, 2016



and refolding of aggregated lysozyme was evaluated. The binding affinities of denatured and native lysozyme to NPs were analyzed and correlated with refolding activity.

All NPs were prepared by pseudoprecipitation polymerization (SI).^{25,26} Hydrophobic *N*-*tert*-butylacrylamide (TBAm), negatively charged acrylic acid (AAc), positively charged *N*-[3-(dimethylamino)propyl] acrylamide (DMAc) and/or *N*-isopropylacrylamide (NIPAm) were incorporated in NPs to evaluate their activity in facilitating resolubilization and refolding (Figure 1a). Table 1 summarizes the monomer feed ratio and

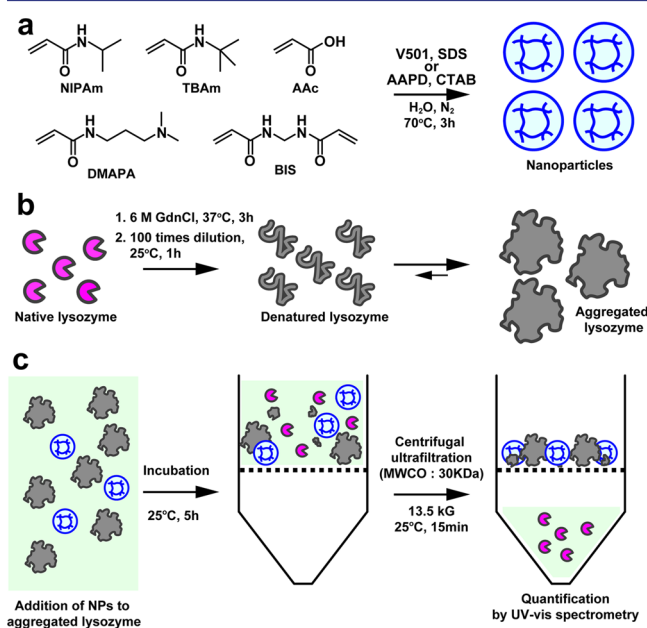


Figure 1. (a) Preparation of polymeric hydrogel nanoparticles. (b) Preparation of aggregated lysozyme by dilution of unfolded lysozyme. (c) Schematic illustration of experiment to test recovery yield of aggregated lysozyme.

hydrodynamic diameter of NPs measured by dynamic light scattering (DLS). All NPs, except NP3, showed relatively fine colloidal stability and narrow size distribution in 100 mM phosphate buffer (pH 7.4). Instability of NP3 may be due to the absence of electrostatic interparticle repulsion.

Denatured lysozyme was prepared by 100 times dilution of 5 mM unfolded lysozyme solution (100 mM tris buffer (pH 8.2), 6 M guanidium hydrochloride) using 100 mM phosphate buffer (pH 7.4) as a dilution buffer (Figure 1b) (SI Figure S1). After

dilution, the solution turned opaque and micrometer objects were observed by DLS, indicating that the denatured lysozymes spontaneously formed aggregates (SI Figures S2 and S3). After 1 h preincubation (25 °C), the diluted solution was filtered by centrifugal ultrafiltration (MWCO: 30 kDa, 13.5 kG, for 15 min at 25 °C) (Figure 1c). It was confirmed that almost all (>90%) lysozyme was trapped by the filter (SI Figure S4). From these results, we concluded that almost all lysozyme formed aggregates larger than 30 kDa after dilution. In contrast, native lysozyme did not form aggregates and passed through the filter almost completely (>99%) (SI Figure S4). Fraction of lysozyme that passed through the filter increased with decreasing of lysozyme concentration in dilution process or with further dilution of aggregated lysozyme (SI Figure S5), indicating lysozyme was kinetically trapped in aggregated state.

To test if aggregated lysozyme can be resolubilized by NPs, NPs (50 μg/mL) were added to the preincubated lysozyme aggregation and the solution mixture was incubated further for 5 h at 25 °C. The solution was filtered using the same conditions as mentioned above, and the amount of lysozyme that passed through the filter (recovery yield of lysozyme) for each NP was quantified by UV-vis spectrometry. Here, we confirmed that NPs were completely trapped by the filter in this step (SI Figure S6).²⁷

The recovery yield of lysozyme by NP1-NP5 is summarized in Figure 2a. When aggregated lysozyme was incubated without NPs in the same conditions, the recovery yield of lysozyme was 6 ± 1%. NPs having only the anionic group (NP1), cationic group (NP2), or hydrophobic group (NP3) did not show a high recovery yield. The recovery yields of NP1, NP2, and NP3 were 4 ± 1%, 6 ± 1%, and 16 ± 2%, respectively. However, NPs having both anionic and hydrophobic group (NP4) showed a large recovery yield, indicating that NP4 effectively facilitated resolubilization of aggregated lysozyme. The recovery yield of NP4 reached 75 ± 5%. In contrast, the recovery yield of a mixture of NP1 and NP3 was 9 ± 2%. It was concluded that each NP required the incorporation of both anionic and hydrophobic groups to effectively facilitate resolubilization of aggregated lysozyme.

The molar ellipticity of the resolubilized lysozyme was investigated by circular dichroism spectroscopy (SI Figure S7). The resolubilized lysozyme showed exactly the same spectrum as native lysozyme, indicating that the resolubilized lysozyme has native structure. Cell lysis activity was comparable with that of native lysozyme (SI Figure S8). These results indicate that the NPs having both anionic and hydrophobic groups facilitate

Table 1. Monomer Composition and Hydrodynamic Diameter and Zeta Potential of NPs^a

	TBAm ^x (mol %)	AAc ^y (mol %)	DMAc ^z (mol %)	diameter (nm)	PdI (-)	zeta potential (mV)	recovery yield (%)
NP1	0	10	0	93	0.10	-13.2	4 ± 1
NP2	0	0	10	120	0.15	9.9	6 ± 1
NP3	70	0	0	N.D.		-4.1	16 ± 2
NP4	70	10	0	103	0.12	-22.8	75 ± 5
NP5	70	0	10	35	0.26	9.3	8 ± 1
NP6	20	10	0	140	0.10	-22.0	9 ± 5
NP7	50	10	0	81	0.10	-13.1	20 ± 2
NP8	70	5	0	85	0.12	-39.9	30 ± 5
NP9	70	20	0	160	0.11	-26.2	47 ± 8
NP10	80	10	0	51	0.06	-33.3	41 ± 10

^aMol% indicates feed ratio in preparation. All NPs contain 10 mol % BIS. Feed ratio of NIPAm (mol %) is 90 X-Y-Z. Diameter and zeta potential were measured in 100 mM and 10 mM phosphate buffer (pH 7.4), respectively.

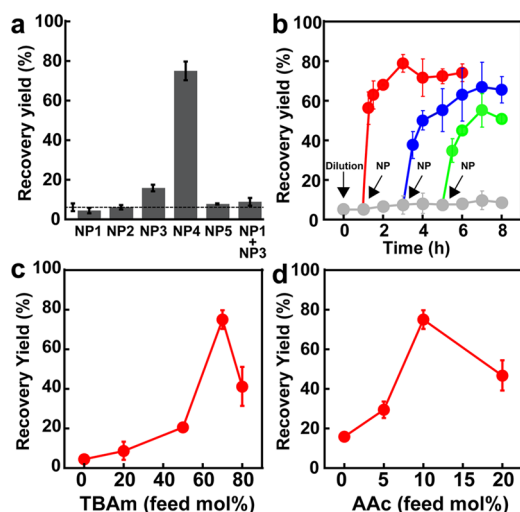


Figure 2. (a) Recovery yield of lysozyme facilitated by NP1–NP5. Dashed line shows recovery yield of lysozyme incubated without NPs. (b) Recovery yield of lysozyme after dilution as a function of time. NP4 was added to aggregated lysozyme at 1 h (red), 3 h (blue), and 5 h (green) and absence of NP (gray). (c) Effect of hydrophobic TBAm feed ratio on facilitating refolding activity. Feed ratio of negatively charged AAc was fixed at 10 mol %. (d) Effect of negatively charged AAc feed ratio on facilitating refolding activity. Feed ratio of hydrophobic TBAm was fixed at 70 mol %.

resolubilization and refolding of aggregated lysozyme. From the amount of refolded lysozyme, it was calculated that 1 g of NPs facilitates resolubilization and refolding of 11 g of aggregated lysozyme.

Refolding kinetics of lysozyme facilitated by NP4 were examined by monitoring the recovery yield as a function of time (Figure 2b). When NPs were added at 1 h, the recovery yield was increased dramatically and reached a maximum in 3 h. The recovery yield and refolding kinetics were slightly decreased with delaying of NP-addition time. It was observed that the size of aggregates increased as a function of time after dilution (SI Figure S2c). Decreased refolding yield and kinetics may due to formation of more stable aggregates during the growing process and/or limitation of the surface area of the aggregates which allows unfolded proteins to dissociate and/or NPs to interact with.¹³

To clarify the importance of population of functional groups, NP6–NP10 were prepared and the recovery yields were evaluated. Effect of feed ratio of hydrophobic TBAm on the recovery yield of lysozyme (feed ratio of AAc was fixed at 10%) is shown in Figure 2c. The recovery yield increased by increasing feed ratio of TBAm when feed ratio of TBAm was less than 70%, indicating the importance of hydrophobic interactions in facilitating refolding of proteins.¹⁰ However, the recovery yield decreased when feed ratio of TBAm was 80%. Effect of feed ratio of negatively charged AAc on the recovery yield of lysozyme (feed ratio of TBAm was fixed at 70%) is shown in Figure 2d. The recovery yield increased when feed ratio of AAc was less than 10% and decreased when feed ratio of AAc was 20%. From these results, we concluded that optimizing population of functional groups is also important to effectively facilitate resolubilization and refolding of aggregated lysozyme.

Binding of denatured lysozyme to NP4 and NP6–NP9 was investigated by quartz crystal microbalance (QCM) (SI). Five microliters of unfolded lysozyme (100 mM tris buffer (pH 8.2), 6 M guanidium hydrochloride) was injected into QCM cells

containing 500 μL of 100 mM phosphate buffer (pH7.4). Binding amounts of denatured lysozyme on NPs immobilized QCM sensor are shown in Figure 3a as a function of lysozyme

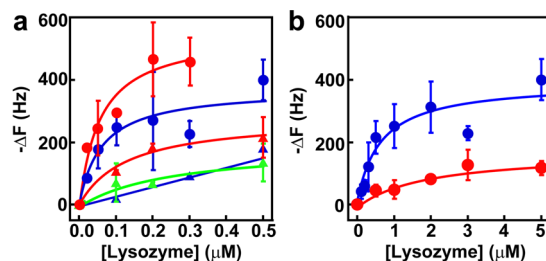


Figure 3. (a) Binding amount of denatured lysozyme on NP4 (red circle), NP6 (green triangle), NP7 (red triangle), NP8 (blue triangle), and NP9 (blue circle) as a function of lysozyme concentration. (b) Binding amount of native lysozyme on NP4 (red circle) and NP9 (blue circle) as a function of lysozyme concentration.

concentration. NP4 and NP9 that effectively facilitated refolding of aggregated lysozyme showed high affinity to denatured lysozyme. Apparent association equilibrium constants (K_a) of NP4 and NP9 to denatured lysozyme, which were estimated by assuming Langmuir type binding, were $(1.7 \pm 0.5) \times 10^7$ and $(1.6 \pm 0.8) \times 10^7 \text{ M}^{-1}$, respectively. (ΔF_{max} of NP4 and NP9 were 554 ± 62 and $373 \pm 57 \text{ Hz}$, respectively.)

However, NP6–NP8, which did not show high facilitation activity, showed a relatively lower affinity to denatured lysozyme than NP4 and NP9. K_a of NP6 and NP7 was $(0.4 \pm 0.3) \times 10^7$ and $(0.7 \pm 0.2) \times 10^7 \text{ M}^{-1}$, respectively. Because of low affinity, K_a of NP8 was not estimated. From these results, we concluded that high affinity of NPs to denatured lysozyme is required to facilitate resolubilization and refolding of aggregated lysozyme.

Facilitation activity of NP9 was 2 times lower than that of NP4, although NP9 also had strong affinity to denatured lysozyme. For further understanding, affinity of NP4 and NP9 to native lysozyme was investigated by QCM (Figure 3b). NP4 and NP9 showed 1–2 order magnitude weaker affinity to native lysozyme than to denatured lysozyme. Stronger affinity of NPs to denatured lysozyme than to native lysozyme may be due to a number of hydrophobic residues of denatured proteins being exposed in solution. NP9 showed 3 times higher K_a to native lysozyme than NP4 (K_a of native lysozyme to NP4 and NP9 were $(0.5 \pm 0.3) \times 10^6$ and $(1.6 \pm 0.7) \times 10^6 \text{ M}^{-1}$, respectively) and 2 times greater binding amount (ΔF_{max} of NP4 and NP9 were 174 ± 37 and $388 \pm 50 \text{ Hz}$, respectively), indicating that weaker interaction with native lysozyme is preferable for NPs to achieve effective facilitation of resolubilization and refolding.

From these results, we concluded that facilitation of resolubilization and refolding of aggregated lysozyme is driven by a strong affinity of NPs to denatured lysozyme as well as a relatively weak affinity with native lysozyme. This behavior is in accordance with the fact that the chaperone proteins show significantly higher affinity to denatured protein than to native protein.¹⁴ NPs have heterogeneous higher dimension structure and sequence of functional monomers, resulting in heterogeneous binding mode between NPs and lysozyme.²⁸ Furthermore, denatured lysozyme that binds to NPs should be a mixture of denatured monomer, dimer, and/or oligomer. However, it is important to note that the apparent affinity observed by QCM experiment clearly correlated with facilitation of resolubilization and refolding activity.

Here, we propose the following mechanisms. Denatured lysozyme form aggregates because of fast intermolecular interaction between denatured lysozymes in the absence of NPs (Figure 4a). This is a kinetically controlled process, and

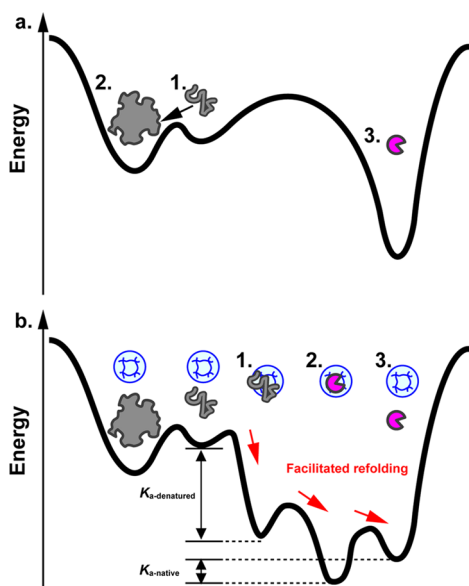


Figure 4. Energy diagram for refolding process of denatured lysozyme after dilution (a) without NPs and (b) with NP4. Denatured lysozyme (a (1)) is trapped in aggregated state (a (2)) and fail to reach native state (a (3)). In the presence of NP4, denatured lysozyme forms a complex with NP4 (b (1)). After refolding (b (2)), native lysozyme is released from NPs (b (3)) as a result of biased affinity of NP4 to denatured and native lysozyme.

thus, the amount of aggregates depends on the concentration of denatured lysozyme (SI Figure S5). When NP4 is added, denatured lysozyme would be captured by NPs because denatured lysozyme have stronger affinity to negatively charged and hydrophobic NP4 than to aggregates that are consisting of positively charged lysozymes (Figure 4b (1)). It can be expected that small denatured-lysozyme can be encapsulated inside the hydrogel particles and isolated from outer environment.^{23,24} Encapsulated lysozymes are thus allowed to reach the most stable native conformation by intramolecular interaction without reaggregate with other denatured proteins (Figure 4b (2)). Since the affinity between native lysozyme and NP4 is weak enough, the refolded lysozyme is automatically released from the NPs or replaced by the other denatured lysozymes, resulting in effective refolding of aggregated protein (Figure 4b (3)). Another possibility is that the captured lysozyme may spontaneously refold soon after being released from NPs. In this pathway, weak affinity between NPs and native proteins is also important in order to prevent competitive inhibition by native proteins. Although, we need further study to completely address the refolding pass-way and to generalize the design rational, we believe that our results provide a direction to design artificial chaperones with high facilitating activity.

■ ASSOCIATED CONTENT

Supporting Information

The Supporting Information is available free of charge on the ACS Publications website at DOI: 10.1021/jacs.5b12600.

Experimental procedures and supporting data (PDF)

■ AUTHOR INFORMATION

Corresponding Author

*yhoshino@chem-eng.kyushu-u.ac.jp

Notes

The authors declare no competing financial interest.

■ ACKNOWLEDGMENTS

Financial support from MEXT (23111716 and 25107726), JSPS (15J04705 and 15H05486) and IMPACT Goda-program is greatly appreciated.

■ REFERENCES

- (1) Muraoka, T.; Adachi, K.; Ui, M.; Kawasaki, S.; Sadhukhan, N.; Obara, H.; Tochio, H.; Shirakawa, M.; Kinbara, K. *Angew. Chem., Int. Ed.* **2013**, *52*, 2430–2434.
- (2) Ganguli, S.; Yoshimoto, K.; Tomita, S.; Sakuma, H.; Matsuoka, T.; Shiraki, K.; Nagasaki, Y. *J. Am. Chem. Soc.* **2009**, *131*, 6549–6553.
- (3) Mancini, R. J.; Lee, J.; Maynard, H. D. *J. Am. Chem. Soc.* **2012**, *134*, 8474–8479.
- (4) Yan, M.; Liu, Z.; Lu, D.; Liu, Z. *Biomacromolecules* **2007**, *8*, 560–565.
- (5) Akiyoshi, K.; Deguchi, S.; Moriguchi, N.; Yamaguchi, S.; Sunamoto, J. *Macromolecules* **1993**, *26*, 3062–3068.
- (6) Nomura, Y.; Ikeda, M.; Yamaguchi, N.; Aoyama, Y.; Akiyoshi, K. *FEBS Lett.* **2003**, *553*, 271–276.
- (7) Sasaki, Y.; Asayama, W.; Niwa, T.; Sawada, S.; Ueda, T.; Taguchi, H.; Akiyoshi, K. *Macromol. Biosci.* **2011**, *11*, 814–820.
- (8) Christopher, M. D. *Nature* **2003**, *426*, 884–890.
- (9) Hartl, F. U.; Hayer-Hartl, M. *Science* **2002**, *295*, 1852–1858.
- (10) Bukau, B.; Horwich, A. L. *Cell* **1998**, *92*, 351–366.
- (11) Doyle, S. M.; Wickner, S. *Trends Biochem. Sci.* **2008**, *34*, 40–48.
- (12) Sweeny, E. A.; Shorter, J. *J. Mol. Biol.* **2015**, DOI: 10.1016/j.jmb.2015.11.016.
- (13) Ranson, N. A.; Dunster, N. J.; Burston, S. G.; Clarke, A. R. *J. Mol. Biol.* **1995**, *250*, 581–586.
- (14) Murai, N.; Taguchi, H.; Yoshida, M. *J. Biol. Chem.* **1995**, *270*, 19957–19963.
- (15) Oguchi, Y.; Kummer, E.; Seyffer, F.; Berynskyy, M.; Anstett, B.; Zahn, R.; Wade, R. C.; Mogk, A.; Bukau, B. *Nat. Struct. Mol. Biol.* **2012**, *19*, 1338–1347.
- (16) Hoshino, Y.; Urakami, T.; Kodama, T.; Koide, H.; Oku, N.; Okahata, Y.; Shea, K. J. *Small* **2009**, *5*, 1562–1568.
- (17) Hoshino, Y.; Koide, H.; Furuya, K.; Haberaecker, W. W.; Lee, H.; Oku, N.; Shea, K. J. *Proc. Natl. Acad. Sci. U. S. A.* **2012**, *109*, 33–38.
- (18) Lee, S. H.; Hoshino, Y.; Randall, A.; Zeng, Z.; Baldi, P.; Doong, R.-A.; Shea, K. J. *J. Am. Chem. Soc.* **2012**, *134*, 15765–15772.
- (19) Yoshimatsu, K.; Lesel, B. K.; Yonamine, Y.; Beierle, J. M.; Hoshino, Y.; Shea, K. J. *Angew. Chem., Int. Ed.* **2012**, *51*, 2405–2408.
- (20) Beierle, J. M.; Yoshimatsu, K.; Chou, B.; Mathews, M. A. A.; Lesel, B. K.; Shea, K. J. *Angew. Chem., Int. Ed.* **2014**, *53*, 9275–9279.
- (21) Cabaleiro-Lago, C.; Quinlan-Pluck, F.; Lynch, I.; Lindman, S.; Minogue, A. M.; Thulin, E.; Walsh, D. M.; Dawson, K. A.; Linse, S. *J. Am. Chem. Soc.* **2008**, *130*, 15437–15443.
- (22) Cabaleiro-Lago, C.; Quinlan-Pluck, F.; Lynch, I.; Dawson, K. A.; Linse, S. *ACS Chem. Neurosci.* **2010**, *1*, 279–287.
- (23) Lyon, L. A.; Smith, M. H. *Macromolecules* **2011**, *44*, 8154–8160.
- (24) Johansson, C.; Gernandt, J.; Bradley, M.; Vincent, B.; Hansson, P. *J. Colloid Interface Sci.* **2010**, *347*, 241–251.
- (25) Pelton, R. *Adv. Colloid Interface Sci.* **2000**, *85*, 1–33.
- (26) Nayak, S.; Lyon, L. A. *Angew. Chem., Int. Ed.* **2005**, *44*, 7686.
- (27) Yue, M.; Hoshino, Y.; Ohshiro, Y.; Imamura, K.; Miura, Y. *Angew. Chem.* **2014**, *126*, 2692–2695.
- (28) Hoshino, Y.; Haberaecker, W. W., III; Kodama, T.; Zeng, Z.; Okahata, Y.; Shea, K. J. *J. Am. Chem. Soc.* **2010**, *132*, 13648.